The Compact Muon Solenoid Experiment

CMS Note

Mailing address: CMS CERN, CH-1211 GENEVA 23, Switzerland

December 20, 2012

Searches for beyond-the-standard model physics in events with a Z boson, jets and missing transverse energy

D. Barge, C. Campagnari, D. Kovalskyi, V. Krutelyov

University of California, Santa Barbara, USA

W. Andrews, G. Cerati, D. Evans, F. Golf, I. MacNeill, S. Padhi, V. Welke, Y. Tu, F. Würthwein, A. Yagil, J. Yoo

University of California, San Diego, USA

L. Bauerdick, K. Burkett, I. Fisk, Y. Gao, O. Gutsche, B. Hooberman, S. Jindariani, J. Linacre, V. Martinez Outschoorn

Fermi National Accelerator Laboratory, Batavia, Illinois, USA

Abstract

This note describes a search for beyond-the-standard model (BSM) physics in events with a leptonically-decaying Z boson, jets, and missing transverse energy (E_T^{miss}). This signature is predicted to occur in several BSM scenarios, for example supersymmetric (SUSY) models. Two search strategies are pursued. The first is an inclusive approach which selects events with at least two jets and large E_T^{miss}, produced in association with the Z$\to \ell\ell$ candidate. The second is a targeted search in which additional requirements are imposed in order to achieve sensitivity to the production of the weakly-coupled SUSY charginos and neutralinos. The main backgrounds of SM Z + jets and $t\bar{t}$ production are estimated with the data-driven E_T^{miss} templates technique and the opposite-flavor subtraction technique, respectively. Additional backgrounds are estimated from simulation, after validation in data control samples. In both the inclusive and targeted analyses, good agreement is observed between the data and predicted background over the full E_T^{miss} range. The results are interpreted in the context of a simplified SUSY model, and used to place constraints on the masses of the electroweak charginos and neutralinos.

Contents

1 Changes w.r.t. previous AN Version

- v6: Updated to full 2012 sample corresponding to 19.3 fb^{-1}.

- v5: **This is the version corresponding to the HCP results**. Added interpretation for the GMSB model (Sec. 8). Added data vs. MC kinematic distributions for the sample with 3 leptons and at least 2 jets, where we observe an excess of data with respect to the MC prediction (App. A).

- v4: Un-blinded the results of the inclusive and targeted analysis, and added an interpretation in the WZ + E_T^{miss} model. Moved the material for the edge analysis to a separate AN (2012/359).

- v3: Added results for the low-E_T^{miss} and high-E_T^{miss} signal regions used for the edge analysis, for the first 5.1 fb^{-1} 2012A+B data.

- v2: Updated to 9.2 fb^{-1} of 53X data and MC (v1 used 5.1 fb^{-1} 52X data and MC).

2 Introduction

This note presents two searches for beyond-the-standard model (BSM) physics in events containing a leptonically-decaying Z boson, jets, and missing transverse energy. This is an update of previous searches performed with 2011 data [1, 2]. The search is based on a data sample of pp collisions collected at $\sqrt{s} = 8$ TeV in 2012, corresponding to an integrated luminosity of 19.3 fb^{-1}.

The production of Z bosons is expected in many BSM scenarios, for example supersymmetric (SUSY) models. In SUSY models with neutralino lightest SUSY particle (LSP), Z bosons may be produced in the decays $\chi_2^0 \to Z\chi_1^0$, where χ_2^0 is the second lightest neutralino and χ_1^0 is the lightest neutralino. In models with gravitino LSP such as gauge-mediated SUSY breaking (GMSB) models, Z bosons may be produced via $\chi_1^0 \to Z\tilde{G}$, where $\tilde{G}$ is the gravitino. Such decays may occur either in the cascade decays of the strongly-produced squarks and gluinos, or via direct production of the electroweak charginos and neutralino. Examples of such processes (see Fig. 1) are:

- strong production: $pp \to \tilde{g}\tilde{g} \to (q\bar{q}\chi_2^0)(q\bar{q}\chi_2^0) \to (q\bar{q}Z\chi_1^0)(q\bar{q}Z\chi_1^0) \to ZZ + 4\,\text{jets} + E_T^{miss}$

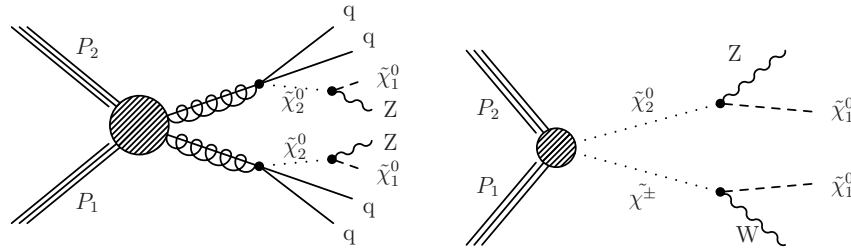- electroweak production: $pp \to \chi_1^\pm \chi_2^0 \to (W\chi_1^0)(Z\chi_1^0) \to WZ + E_T^{miss}$

Figure 1: Examples of BSM physics signatures targeted in this search. In the left diagram, Z bosons are produced in the cascade decays of the strongly-interacting gluinos. In the right diagram, a Z boson is produced via direct production of the weakly-coupled charginos and neutralinos.

We thus pursue two strategies. The first is an inclusive strategy which selects events with a Z$\to \ell\ell$ candidate, at least two jets, and large E_T^{miss}. This strategy is useful for targeting, e.g., the production of Z bosons in the cascade decays of strongly-interacting particles as depicted in Fig. 1 (left). In the second strategy, we impose additional requirements which strongly suppress the backgrounds while retaining high efficiency for events with Z bosons produced via direct production of the weakly-coupled charginos and neutralinos. These two strategies are referred to as the "inclusive search" and the "targeted search," respectively.

After selecting events with jets and a Z$\to \ell^+\ell^-$ ($\ell = e, \mu$) candidate, the dominant background consists of SM Z production accompanied by jets from initial-state radiation (Z + jets). The E_T^{miss} in Z + jets events arises primarily when jet energies are mismeasured. The Z + jets cross section is several orders of magnitude larger than our signal, and the artificial E_T^{miss} is not necessarily well reproduced in simulation. Therefore, the critical prerequisite to a discovery of BSM physics in the $Z + \text{jets} + E_T^{miss}$ final state is to establish that a potential excess is not due to SM Z + jets production accompanied by artificial E_T^{miss} from jet mismeasurements. In this note,

the $Z + \mathrm{jets}$ background is estimated with the E_T^{miss} templates technique, in which the artificial E_T^{miss} in $Z + \mathrm{jets}$ events is modeled using a $\gamma + \mathrm{jets}$ control sample. The second background category consists of processes which produce leptons with uncorrelated flavor. These "flavor-symmetric" (FS) backgrounds, which are dominated by $t\bar{t}$ but also contain WW, DY$\rightarrow \tau\tau$ and single top processes, are estimated using a data control sample of eμ events. Additional backgrounds from WZ and ZZ production are estimated from MC, after validation of the MC modeling of these processes using 3-lepton and 4-lepton data control samples.

3 Datasets and Triggers

In this section we list the datasets, triggers, and MC samples used in the analysis. For selecting signal events, we use dilepton triggers in the DoubleElectron, DoubleMu, and MuEG datasets. An event in the ee final state is required to pass the dielectron trigger, a $\mu\mu$ event is required to pass the dimuon trigger, while an eμ event is required to pass at least one of the two $e - \mu$ cross triggers. The efficiencies of the ee, $\mu\mu$ and eμ triggers with respect to the offline selection have been measured as 0.95 ± 0.03, 0.88 ± 0.03, and 0.92 ± 0.03, respectively [6]. These trigger efficiencies were measured with the first 5.1 fb^{-1} and will be updated with the full data sample. Preliminary measurements of the trigger efficiency with the full sample show consistent results within $\sim 1 - 2\%$. A sample of $\gamma + \text{jets}$ events, used as a control sample to estimate the $Z + \text{jets}$ background, is selected using a set of single photon triggers. The golden prompt reco json corresponding to 19.3 fb^{-1} is used.

- Datasets

    - DoubleElectron
    - DoubleMu
    - MuEG

- Datasets

    - Run2012A-13Jul2012-v1
    - Run2012A-recover-06Aug2012-v1
    - Run2012B-13Jul2012-v1
    - Run2012C-24Aug2012-v1
    - Run2012C-PromptReco-v2
    - MuEG_Run2012D-PromptReco-v1

- Triggers

    - HLT_Mu17_Mu8_v*
    - HLT_Mu17_Ele8_CaloIdT_CaloIsoVL_TrkIdVL_TrkIsoVL_v*
    - HLT_Mu8_Ele17_CaloIdT_CaloIsoVL_TrkIdVL_TrkIsoVL*
    - HLT_Ele17_CaloIdT_CaloIsoVL_TrkIdVL_TrkIsoVL_Ele8_CaloIdT_CaloIsoVL_TrkIdVL_TrkIsoVL_v*
    - HLT_Photon22_R9Id90_HE10_Iso40_EBOnly_v*
    - HLT_Photon36_R9Id90_HE10_Iso40_EBOnly_v*
    - HLT_Photon50_R9Id90_HE10_Iso40_EBOnly_v*
    - HLT_Photon75_R9Id90_HE10_Iso40_EBOnly_v*
    - HLT_Photon90_R9Id90_HE10_Iso40_EBOnly_v*

Table 1: List of MC samples.

Process	Dataset Name	Cross Section [pb]
$Z + \text{jets}$	/DYJetsToLL_M-50_TuneZ2Star_8TeV-madgraph-tarball/Summer12_DR53X-PU_S10_START53_V7A-v1/AODSIM	3532.8
$t\bar{t}$	/TTJets_MassiveBinDECAY_TuneZ2star_8TeV-madgraph-tauola/Summer12_DR53X-PU_S10_START53_V7A-v1/AODSIM	225.2
ZZ	/ZZJetsTo4L_TuneZ2star_8TeV-madgraph-tauola/Summer12_DR53X-PU_S10_START53_V7A-v1/AODSIM	0.1769
	/ZZJetsTo2L2Q_TuneZ2star_8TeV-madgraph-tauola/Summer12_DR53X-PU_S10_START53_V7A-v1/AODSIM	2.4487
	/ZZJetsTo2L2Nu_TuneZ2star_8TeV-madgraph-tauola/Summer12_DR53X-PU_S10_START53_V7A-v3/AODSIM	0.3648
WZ	/WZJetsTo3LNu_TuneZ2_8TeV-madgraph-tauola/Summer12_DR53X-PU_S10_START53_V7A-v1/AODSIM	1.0575
	/WZJetsTo2L2Q_TuneZ2star_8TeV-madgraph-tauola/Summer12_DR53X-PU_S10_START53_V7A-v1/AODSIM	2.206
WW	/WWJetsTo2L2Nu_TuneZ2star_8TeV-madgraph-tauola/Summer12_DR53X-PU_S10_START53_V7A-v1/AODSIM	5.8123
single top	/T_tW-channel-DR_TuneZ2star_8TeV-powheg-tauola/Summer12_DR53X-PU_S10_START53_V7A-v1/AODSIM	11.177
	/Tbar_tW-channel-DR_TuneZ2star_8TeV-powheg-tauola/Summer12_DR53X-PU_S10_START53_V7A-v1/AODSIM	11.177
ttV	/TTZJets_8TeV-madgraph_v2/Summer12_DR53X-PU_S10_START53_V7A-v1/AODSIM	0.208
	/TTWJets_8TeV-madgraph/Summer12_DR53X-PU_S10_START53_V7A-v1/AODSIM	0.232
VVV	/ZZZNoGstarJets_8TeV-madgraph/Summer12_DR53X-PU_S10_START53_V7A-v1/AODSIM	0.01922
	/WWWJets_8TeV-madgraph/Summer12_DR53X-PU_S10_START53_V7A-v1/AODSIM	0.08217
	/WWZNoGstarJets_8TeV-madgraph/Summer12_DR53X-PU_S10_START53_V7A-v1/AODSIM	0.0633

4 Selection

In this section, we list the event selection, electron and muon objects selections, jets, E_T^{miss}, and b-tagging selections used in this analysis. These selections are based on those recommended by the relevant POG's.

4.1 Event Selection

We require the presence of at least one primary vertex satisfying the standard quality criteria; namely, vertex is not fake, $ndf \geq 4$, $\rho < 2$ cm, and $|z| < 24$ cm.

4.2 Lepton Selection

Because $Z \to \ell\ell$ ($\ell = e, \mu$) is a final state with very little background, we restrict ourselves to events in which the Z boson decays to electrons or muons only. Therefore opposite sign leptons passing the identification and isolation requirements described below are required in each event.

- $p_T > 20$ GeV and $|\eta| < 2.4$;

- Opposite-sign same-flavor (SF) ee and $\mu\mu$ lepton pairs (opposite-flavor (OF) eμ lepton pairs are retained in a control sample used to estimate the FS contribution);

- For SF events, the dilepton invariant mass is required to be consistent with the Z mass; namely $81 < m_{\ell\ell} < 101$ GeV.

4.2.1 Electron Selection

The electron selection is the loose working point recommended by the E/gamma POG, as documented at [3]. Electrons with $p_T > 20$ GeV and $|\eta| < 2.4$ are considered. We use PF-based isolation with a cone size of $\Delta R < 0.3$, using the effective area rho corrections documented at [4], and we require a relative isolation < 0.15. Electrons in the transition region defined by $1.4442 < |\eta_{SC}| < 1.566$ are rejected. Electrons with a selected muon with $p_T > 10$ GeV within $\Delta R < 0.1$ are rejected. The electron selection requirements are listed in Table 2 for completeness.

Table 2: Summary of the electron selection requirements.

Quantity	Barrel	Endcap
$\delta\eta$	< 0.007	< 0.009
$\delta\phi$	< 0.15	< 0.10
$\sigma_{i\eta i\eta}$	< 0.01	< 0.03
H/E	< 0.12	< 0.10
d_0 (w.r.t. 1st good PV)	< 0.02 cm	< 0.02 cm
d_z (w.r.t. 1st good PV)	< 0.2 cm	< 0.2 cm
$|1/E - 1/P|$	< 0.05 GeV^{-1}	< 0.05 GeV^{-1}
PF isolation / p_T	< 0.15	< 0.15
conversion rejection: fit probability	$< 10^{-6}$	$< 10^{-6}$
conversion rejection: missing hits	≤ 1	≤ 1

4.2.2 Muon Selection

We use the tight muon selection recommended by the muon POG, as documented at [5]. Muons with $p_T > 20$ GeV and $|\eta| < 2.4$ are considered. We use PF-based isolation with a cone size of $\Delta R < 0.3$, using the $\Delta\beta$ PU correction scheme, and we require a relative isolation of < 0.15. The muon selection requirements are listed in Table 3 for completeness.

4.3 Photons

As will be explained later, it is not essential that we select real photons. What is needed are jets that are predominantly electromagnetic, well measured in the ECAL, and hence less likely to contribute to fake MET. We select photons with:

Table 3: Summary of the muons selection requirements.

Quantity	Requirement
muon type	global muon and PF muon
χ^2/ndf	< 10
muon chamber hits	≥ 1
matched stations	≥ 2
d_0 (w.r.t. 1st good PV)	< 0.02 cm
d_z (w.r.t. 1st good PV)	< 0.5 cm
pixel hits	≥ 1
tracker layers	≥ 5

- $p_T > 22$ GeV

- $|\eta| < 2$

- $H/E < 0.1$

- No matching pixel track (pixel veto)

- There must be a pfjet of $p_T > 10$ GeV matched to the photon within $dR < 0.3$. The matched jet is required to have a neutral electromagnetic energy fraction of at least 70%.

- We require that the pfjet p_T matched to the photon satisfy (pfjet p_T - photon p_T) > -5 GeV. This removes a few rare cases in which "overcleaning" of a pfjet generates fake MET.

- We also match photons to calojets and require (calojet p_T - photon p_T) > -5 GeV (the same requirement used for pfjets). This is to remove other rare cases in which fake energy is added to the photon object but not the calojet.

- We reject photons which have an electron of at least $p_T > 10$ GeV within $dR < 0.2$ in order to reject conversions from electrons from W decays which are accompanied by real MET.

- We reject photons which are aligned with the MET to within 0.14 radians in phi.

4.4 MET

We use pfmet, henceforth referred to simply as $\mathrm{E}_T^{\mathrm{miss}}$.

4.5 Jets

- PF jets with L1FastL2L3 corrections (MC), L1FastL2L3residual corrections (data), using the 52X jet energy corrections

- $|\eta| < 2.5$

- Passes loose PFJet ID

- $p_T > 30$ GeV for determining the jet multiplicity, $p_T > 15$ GeV for calculation of H_T

- For the creation of photon templates, the jet matched to the photon passing the photon selection described above is vetoed

- For the dilepton sample, jets are vetoed if they are within $\Delta R < 0.4$ from any lepton $p_T > 20$ GeV passing analysis selection

7

5 Data vs. MC Comparison in Preselection Region

In this section we compare the data and MC samples passing the selection described in Sec. 4 In the following, the MC is reweighted to match the data distribution of number of reconstructed primary vertices. The trigger efficiencies of Sec. 3 are applied. In all plots, the last bin contains the overflow.

We begin by counting the inclusive Z yields. Here we require the presence of two selected leptons without any additional requirements on jets or E_T^{miss}. In Fig. 2 the distribution of dilepton invariant mass in the ee and $\mu\mu$ channels is displayed. In Table 4 the yields for selected dilepton events in the Z mass window are indicated. Good data vs. MC agreement is observed, within the systematic uncertainties of integrated luminosity (4.5%), trigger efficiency (3%), $Z + \text{jets}$ and $t\bar{t}$ cross sections.
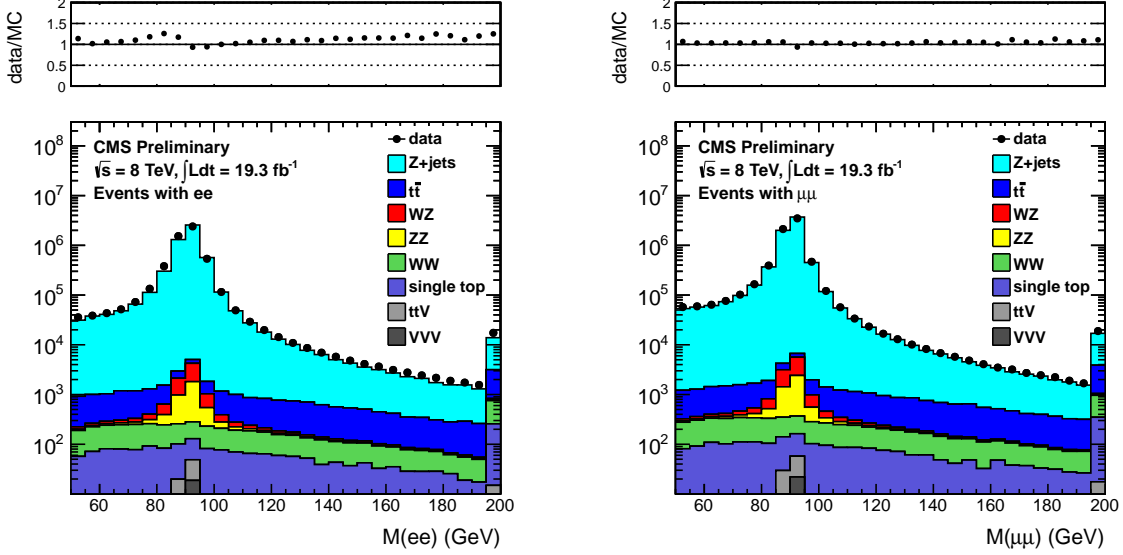

Figure 2: Dilepton mass distribution for events with two selected leptons in the ee (left) and $\mu\mu$ (right) final states.

Table 4: Data and Monte Carlo yields for events with two selected leptons in the Z mass window.

Sample	ee	$\mu\mu$	eμ	total
$Z + \text{jets}$	4735966.0 ± 3483.0	6507980.5 ± 3928.4	2270.5 ± 75.1	11246217.0 ± 5250.7
$t\bar{t}$	3312.7 ± 47.4	4192.1 ± 51.2	7535.8 ± 70.3	15040.6 ± 99.0
WZ	4306.1 ± 7.5	5647.2 ± 8.3	113.5 ± 1.1	10066.8 ± 11.2
ZZ	2713.5 ± 5.7	3582.7 ± 6.2	10.8 ± 0.1	6307.0 ± 8.4
WW	609.5 ± 6.2	812.3 ± 6.8	1408.2 ± 9.2	2830.0 ± 13.0
single top	314.6 ± 12.3	404.1 ± 13.3	698.4 ± 18.0	1417.0 ± 25.5
ttV	56.6 ± 1.1	69.9 ± 1.2	21.3 ± 0.7	147.8 ± 1.7
VVV	26.3 ± 0.3	33.3 ± 0.4	6.8 ± 0.2	66.3 ± 0.6
total SM MC	4747305.0 ± 3483.4	6522722.0 ± 3928.8	12065.3 ± 104.8	11282092.3 ± 5251.7
data	4828868	6434546	12872	11276286

139 We next define the preselection region for the inclusive search using the following requirements:

140 • Number of jets ≥ 2;

141 • Same flavor dileptons (opposite flavor yields will be shown since they are used in data for the FS background
142 estimation);

143 • Dilepton invariant mass $81 < m_{\ell\ell} < 101$ GeV.

144 The dilepton mass distributions in the preselection region of the inclusive search (without the dilepton mass re-
145 quirement applied) for the ee and $\mu\mu$ final states are shown in Figure 3. In Table 5 the data and MC yields in the
146 inclusive preselection region are indicated. Good data vs. MC agreement is observed.
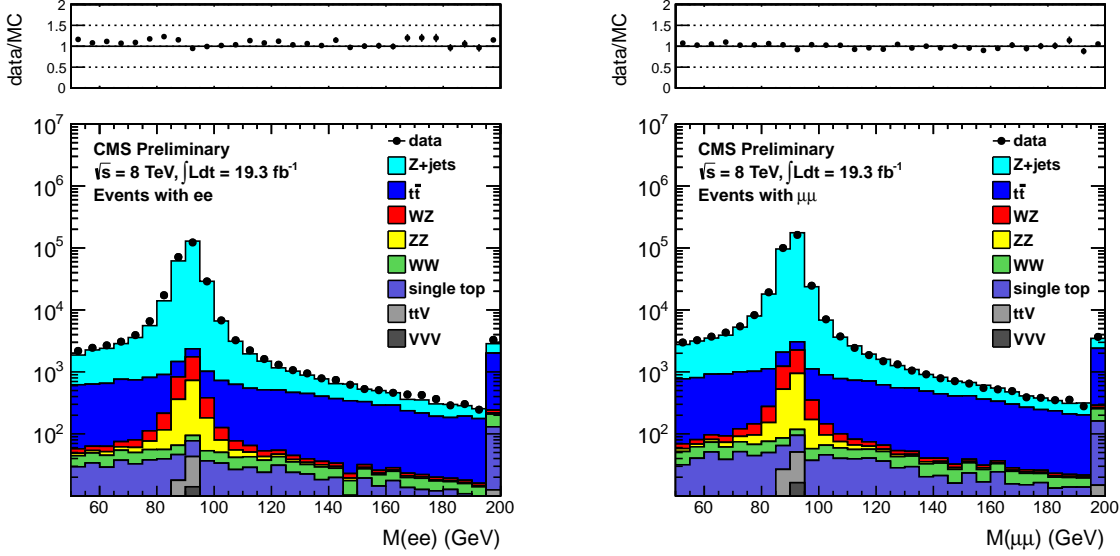

Figure 3: Dilepton mass distribution for events in the preselection region of the inclusive search in the ee (left) and
$\mu\mu$ (right) final states.

Table 5: Data and MC yields in the preselection region of the inclusive search.

Sample	ee	$\mu\mu$	eμ	total
Z + jets	228270.2 ± 751.0	306348.9 ± 836.3	125.3 ± 17.5	534744.4 ± 1124.2
$t\bar{t}$	2561.2 ± 41.6	3240.6 ± 45.0	5849.1 ± 61.8	11650.9 ± 87.1
WZ	1790.4 ± 4.9	2308.4 ± 5.4	22.4 ± 0.5	4121.2 ± 7.3
ZZ	1116.9 ± 3.8	1453.3 ± 4.2	2.5 ± 0.1	2572.7 ± 5.6
WW	68.6 ± 2.1	89.1 ± 2.3	156.7 ± 3.0	314.4 ± 4.3
single top	126.7 ± 7.7	153.4 ± 8.2	276.4 ± 11.2	556.6 ± 15.9
ttV	54.4 ± 1.1	67.5 ± 1.1	19.7 ± 0.7	141.6 ± 1.7
VVV	19.3 ± 0.3	24.4 ± 0.3	3.4 ± 0.1	47.1 ± 0.5
total SM MC	234007.8 ± 752.3	313685.7 ± 837.6	6455.5 ± 65.3	554149.1 ± 1127.7
data	239661	304953	6279	550893

147 We next define the preselection region for the targeted search by adding the following requirements:

148 • Veto events containing a b-tagged jet;

149 • Dijet invariant mass $70 < m_{jj} < 110$ GeV;

150 • Veto events containing a third selected lepton (electron or muon) with $p_T > 10$ GeV;

151 The rejection of events with a b-tagged jet strongly suppresses the $t\bar{t}$ background, which is the dominant back-
152 ground in the inclusive search after requiring large E_T^{miss}. The requirement that the jet pair is consistent with orig-
153 inating from W/Z decay is motivated by the fact that we are searching for signatures producing $V(jj)Z(\ell\ell)+E_T^{miss}$;
154 this requirement suppresses the $Z + jets$ and $t\bar{t}$ backgrounds. The veto of events containing a third electron or
155 muon suppresses the WZ background, and also serves to make this analyis exclusive with respect to searches in
156 the trilepton final state.

157 The dilepton mass distributions in the preselection region of the targeted search (without the dilepton mass re-
158 quirement applied) for the ee and $\mu\mu$ final states are shown in Figure 4. In Table 6 the data and MC yields in the
159 preselection region are indicated. Good data vs. MC agreement is observed. We also show the distribution of dijet
160 mass in the targeted preselection (with the requirement on this quantity removed) in Fig. 5, which demonstrates
161 that the MC does a reasonable job of modeling this quantity.
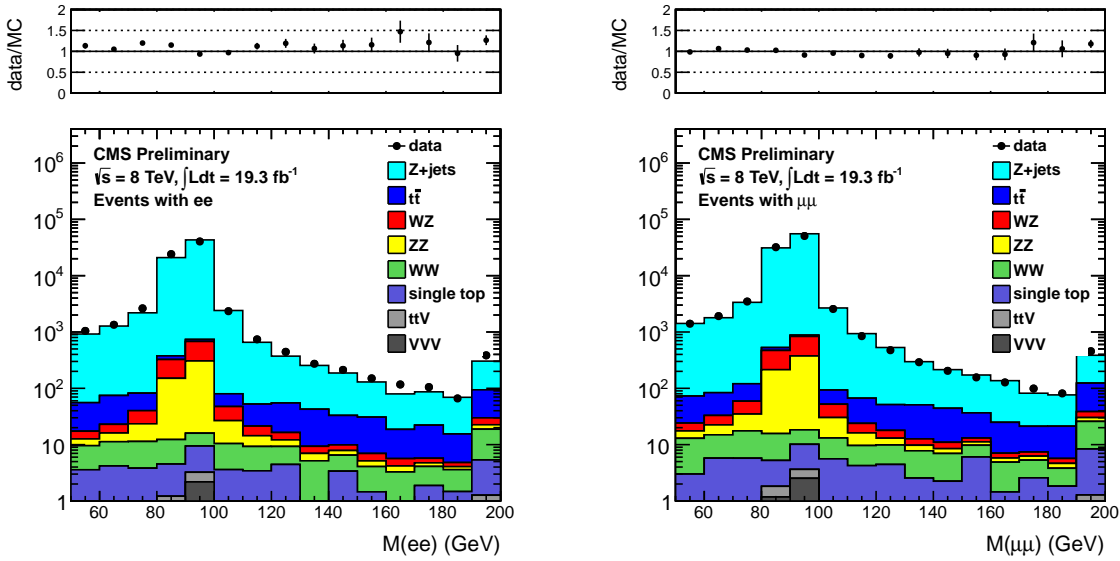

Figure 4: Dilepton mass distribution for events in the preselection region of the targeted search in the ee (left) and
$\mu\mu$ (right) final states.

Table 6: Data and MC yields in the preselection region of the targeted search.

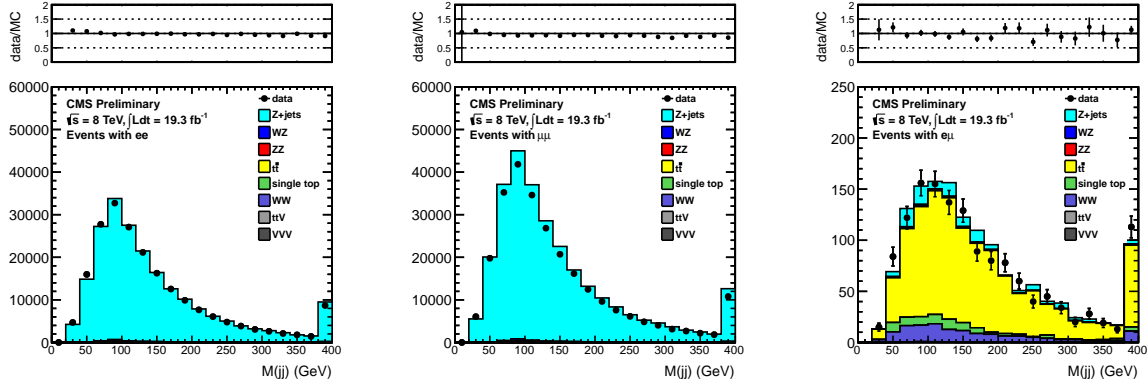| Sample	ee	$\mu\mu$	eμ	total
$Z + jets$	63014.6 ± 392.2	85083.6 ± 438.2	27.1 ± 7.8	148125.3 ± 588.1
$t\bar{t}$	106.0 ± 8.5	102.9 ± 7.9	220.5 ± 12.0	429.4 ± 16.7
WZ	546.8 ± 2.8	712.9 ± 3.0	3.5 ± 0.2	1263.2 ± 4.1
ZZ	428.3 ± 2.4	554.0 ± 2.6	0.4 ± 0.1	982.7 ± 3.5
WW	14.2 ± 0.9	18.0 ± 1.0	33.4 ± 1.4	65.6 ± 2.0
single top	9.8 ± 2.2	10.5 ± 2.1	17.8 ± 2.8	38.1 ± 4.2
ttV	1.6 ± 0.2	1.7 ± 0.2	0.9 ± 0.1	4.2 ± 0.3
VVV	2.9 ± 0.1	3.7 ± 0.1	0.9 ± 0.1	7.5 ± 0.2
total SM MC	64124.2 ± 392.3	86487.3 ± 438.3	304.5 ± 14.7	150916.0 ± 588.4
data	64385	82426	306	147117

Figure 5: Distributions of dijet mass for the targeted preselection in the ee (left), $\mu\mu$ (middle) and eμ (right) final state.

6 Background Estimation Techniques

In this section we describe the techniques used to estimate the SM backgrounds in our signal regions defined by requirements of large E_T^{miss}. The SM backgrounds fall into three categories:

- Z + jets : this is the dominant background after the preselection. The E_T^{miss} in Z + jets events is estimated with the "E_T^{miss} templates" technique described in Sec. 6.1;

- Flavor-symmetric (FS) backgrounds: this category includes processes which produces 2 leptons of uncorrelated flavor. It is dominated by $t\bar{t}$ but also contains Z$\rightarrow \tau\tau$, WW, and single top processes. This is the dominant contribution in the signal regions, and it is estimated using a data control sample of eμ events as described in Sec. 6.2;

- WZ and ZZ backgrounds: this background is estimated from MC, after validating the MC modeling of these processes using data control samples with jets and exactly 3 leptons (WZ control sample) and exactly 4 leptons (ZZ control sample) as described in Sec. 6.3;

6.1 Estimating the Z + jets Background with E_T^{miss} Templates

The premise of this data driven technique is that E_T^{miss} in Z + jets events is produced by the hadronic recoil system and *not* by the leptons making up the Z. Therefore, the basic idea of the E_T^{miss} template method is to measure the E_T^{miss} distribution in a control sample which has no true MET and the same general attributes regarding fake MET as in Z + jets events. We thus use a sample of γ + jets events, since both Z + jets and γ + jets events consist of a well-measured object recoiling against hadronic jets.

For selecting photon-like objects, the very loose photon selection described in Sec. 4.3 is used. It is not essential for the photon sample to have high purity. For our purposes, selecting jets with predominantly electromagnetic energy deposition in a good fiducial volume suffices to ensure that they are well measured and do not contribute to fake E_T^{miss}. The γ + jets events are selected with a suite of single photon triggers with p_T thresholds varying from 22–90 GeV. The events are weighted by the trigger prescale such that γ + jets events evenly sample the conditions over the full period of data taking. There remains a small difference in the PU conditions in the γ + jets vs. Z + jets samples due to the different dependencies of the γ vs. Z isolation efficiencies on PU. To account for this, we reweight the γ + jets samples to match the distribution of reconstructed primary vertices in the Z + jets sample.

To account for kinematic differences between the hadronic systems in the control vs. signal samples, we measure the E_T^{miss} distributions in the γ + jets sample in bins of the number of jets and the scalar sum of jet transverse energies (H_T). These E_T^{miss} templates are extracted separately from the 5 single photon triggers with thresholds 22, 36, 50, 75, and 90 GeV, so that the templates are effectively binned in photon p_T. All E_T^{miss} distributions are normalized to unit area to form "MET templates". The prediction of the MET in each Z event is the template which corresponds to the N_{jets}, H_T, and Z p_T in the Z + jets event. The prediction for the Z sample is simply the sum of all such templates. All templates are displayed in App. B.

After preselection, there is a small contribution from backgrounds other than Z + jets . To correct for this, the E_T^{miss} templates prediction is scaled such that the total background prediction matches the observed data yield in the E_T^{miss} 0–60 GeV region. Because the non-Z + jets impurity in the low E_T^{miss} region after preselection is very small, this results in scaling factors of 0.985 (0.995) for the inclusive (targeted) search.

6.2 Estimating the Flavor-Symmetric Background with eμ Events

In this subsection we describe the background estimate for the FS background. Since this background produces equal rates of same-flavor (SF) ee and $\mu\mu$ lepton pairs as opposite-flavor (OF) eμ lepton pairs, the OF yield can be used to estimate the SF yield, after correcting for the different electron vs. muon offline selection efficiencies and the different efficiencies for the ee, $\mu\mu$, and eμ triggers.

An important quantity needed to translate from the OF yield to a prediction for the background in the SF final state is the ratio $R_{\mu e} = \epsilon_\mu/\epsilon_e$, where ϵ_μ (ϵ_e) indicates the offline muon (electron) selection efficiency. This quantity can be extracted from data using the observed Z$\to \mu\mu$ and Z$\to$ee yields in the preselection region, after correcting for the different trigger efficiencies.

Hence we define:

- $N_{ee}^{\text{trig}} = \epsilon_{ee}^{\text{trig}} N_{ee}^{\text{offline}}$,

- $N_{\mu\mu}^{\text{trig}} = \epsilon_{\mu\mu}^{\text{trig}} N_{\mu\mu}^{\text{offline}}$,

- $N_{e\mu}^{\text{trig}} = \epsilon_{e\mu}^{\text{trig}} N_{e\mu}^{\text{offline}}$.

Here $N_{\ell\ell}^{\text{trig}}$ denotes the number of selected Z events in the $\ell\ell$ channel passing the offline and trigger selection (in other words, the number of recorded and selected events), $\epsilon_{\ell\ell}^{\text{trig}}$ is the trigger efficiency, and $N_{\ell\ell}^{\text{offline}}$ is the number of events that would have passed the offline selection if the trigger had an efficiency of 100%. Thus we calculate the quantity:

$$R_{\mu e} = \sqrt{\frac{N_{\mu\mu}^{\text{offline}}}{N_{ee}^{\text{offline}}}} = \sqrt{\frac{N_{\mu\mu}^{\text{trig}}/\epsilon_{\mu\mu}^{\text{trig}}}{N_{ee}^{\text{trig}}/\epsilon_{ee}^{\text{trig}}}} = \sqrt{\frac{304953/0.88}{239661/0.95}} = 1.17 \pm 0.07. \tag{1}$$

Here we have used the Z$\to \mu\mu$ and Z$\to$ee yields from Table 5 and the trigger efficiencies quoted in Sec. 3. The indicated uncertainty is due to the 3% uncertainties in the trigger efficiencies. The predicted yields in the ee and $\mu\mu$ final states are calculated from the observed eμ yield as

- $N_{ee}^{\text{predicted}} = \frac{N_{e\mu}^{\text{trig}}}{\epsilon_{e\mu}^{\text{trig}}} \frac{\epsilon_{ee}^{\text{trig}}}{2R_{\mu e}} = \frac{N_{e\mu}^{\text{trig}}}{0.92} \frac{0.95}{2\times 1.17} = (0.44 \pm 0.05) \times N_{e\mu}^{\text{trig}}$,

- $N_{\mu\mu}^{\text{predicted}} = \frac{N_{e\mu}^{\text{trig}}}{\epsilon_{e\mu}^{\text{trig}}} \frac{\epsilon_{\mu\mu}^{\text{trig}} R_{\mu e}}{2} = \frac{N_{e\mu}^{\text{trig}}}{0.95} \frac{0.88\times 1.17}{2} = (0.54 \pm 0.07) \times N_{e\mu}^{\text{trig}}$,

and the predicted yield in the combined ee and $\mu\mu$ channel is simply the sum of these two predictions:

- $N_{ee+\mu\mu}^{\text{predicted}} = (0.98 \pm 0.06) \times N_{e\mu}^{\text{trig}}$.

Note that the relative uncertainty in the combined ee and $\mu\mu$ prediction is smaller than those for the individual ee and $\mu\mu$ predictions because the uncertainty in $R_{\mu e}$ cancels when summing the ee and $\mu\mu$ predictions.

To improve the statistical precision of the FS background estimate, we remove the requirement that the eμ lepton pair falls in the Z mass window. Instead we scale the eμ yield by K, the efficiency for eμ events to satisfy the Z mass requirement, extracted from simulation. In Fig. 6 we display the value of K in data and simulation, for a variety of E_T^{miss} requirements, for the inclusive analysis. Based on this we chose $K = 0.14 \pm 0.02$ for the lower E_T^{miss} regions, $K = 0.14 \pm 0.04$ for the $E_T^{\text{miss}} > 200$ GeV region, and $K = 0.14 \pm 0.09$ for $E_T^{\text{miss}} > 300$ GeV, where the larger uncertainties reflect the reduced statistical precision at large E_T^{miss}. The corresponding plot for the targeted analysis, including the b-veto, is displayed in Fig. 7. Based on this we chose $K = 0.13 \pm 0.02$ for all E_T^{miss} regions up to $E_T^{\text{miss}} > 150$ GeV. For the $E_T^{\text{miss}} > 200$ GeV region we choose $K = 0.13 \pm 0.05$, due to the reduced statistical precision.
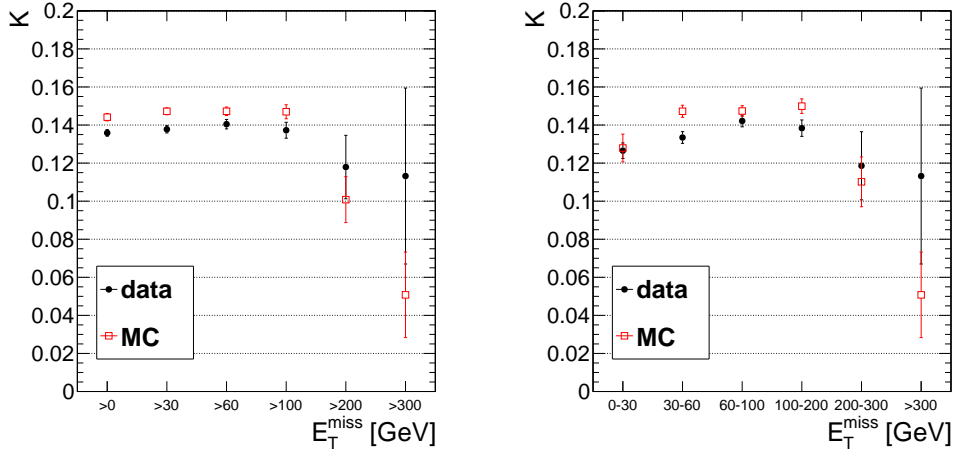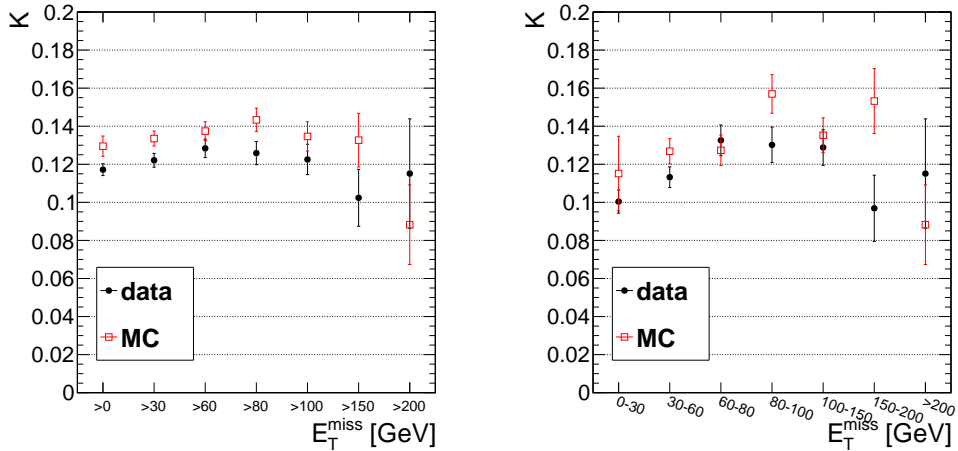
Figure 6: The efficiency for eμ events to satisfy the dilepton mass requirement, K, in data and simulation for inclusive E_T^{miss} intervals (left) and exclusive E_T^{miss} intervals (right) for the inclusive analysis.

Figure 7: The efficiency for eμ events to satisfy the dilepton mass requirement, K, in data and simulation for inclusive E_T^{miss} intervals (left) and exclusive E_T^{miss} intervals (right) for the targeted analysis, including the b-veto. Based on this we chose $K = 0.13 \pm 0.02$ for the E_T^{miss} regions up to $E_T^{miss} > 100$ GeV. For higher E_T^{miss} regions we chose $K = 0.13 \pm 0.07$.

13

6.3 Estimating the WZ and ZZ Background with MC

Backgrounds from $W(\ell\nu)Z(\ell\ell)$ where the W lepton is not identified or is outside acceptance, and $Z(\nu\nu)Z(\ell\ell)$, are estimated from simulation. The MC modeling of these processes is validated by comparing the MC predictions with data in control samples with exactly 3 leptons (WZ control sample) and exactly 4 leptons (ZZ control sample). The critical samples are the WZJetsTo3LNu and ZZJetsTo4L, listed in Table 1 (the WZJetsTo2L2Q, ZZJetsTo2L2Q, and ZZJetsTo2L2Nu samples are also used in this analysis but their contribution to the 3-lepton and 4-lepton control samples is negligible).

6.3.1 WZ Validation Studies

A pure WZ sample can be selected in data with the requirements:

- Exactly 3 $p_T > 20$ GeV leptons passing analysis identication and isolation requirements,

- 2 of the 3 leptons must fall in the Z window 81-101 GeV,

- $E_T^{miss} > 50$ GeV (to suppress DY).

The data and MC yields passing the above selection are in Table 7. The inclusive yields (without any jet requirements) agree within 13%, which is consistent within the uncertainty in the CMS measured WZ cross section (17%). A data vs. MC comparison of kinematic distributions (jet multiplicity, E_T^{miss}, Z p_T) is given in Fig. 8. High E_T^{miss} values in WZ and ZZ events arise from highly boosted W or Z bosons that decay leptonically, and we therefore check that the MC does a reasonable job of reproducing the p_T distributions of the leptonically decaying Z. While the inclusive WZ yields are in reasonable agreement, we observe an excess in data in events with at least 2 jets, corresponding to the jet multiplicity requirement in our preselection. We observe 106 events in data while the MC predicts 62 ± 1.5 (stat), representing an excess of 71%, as indicated in Table 8. This excess will be studied further. For the time being, based on these studies we currently assess an uncertainty of 70% on the WZ yield. A data vs. MC comparison of several kinematic quantities in the sample with 3 leptons and at least 2 jets can be found in App. A.

Table 7: Data and Monte Carlo yields passing the WZ preselection.

Sample	ee	$\mu\mu$	eμ	total
WZ	244.9 ± 1.6	317.9 ± 1.8	17.0 ± 0.4	579.7 ± 2.4
Z + jets	2.5 ± 2.0	6.4 ± 3.9	0.0 ± 0.0	8.9 ± 4.3
ZZ	5.3 ± 0.0	7.1 ± 0.1	0.4 ± 0.0	12.8 ± 0.1
$t\bar{t}$	2.5 ± 1.3	6.7 ± 2.0	7.5 ± 2.1	16.7 ± 3.2
single top	0.0 ± 0.0	0.5 ± 0.5	0.0 ± 0.0	0.5 ± 0.5
WW	0.0 ± 0.0	0.1 ± 0.1	0.2 ± 0.1	0.3 ± 0.1
ttV	8.6 ± 0.4	10.3 ± 0.4	2.5 ± 0.2	21.5 ± 0.7
VVV	3.4 ± 0.1	4.3 ± 0.1	0.6 ± 0.1	8.3 ± 0.2
tot SM MC	267.1 ± 2.9	353.3 ± 4.7	28.2 ± 2.2	648.6 ± 6.0
data	312	391	50	753

14

Table 8: Data and Monte Carlo yields passing the WZ preselection and $N_{\text{jets}} \geq 2$.

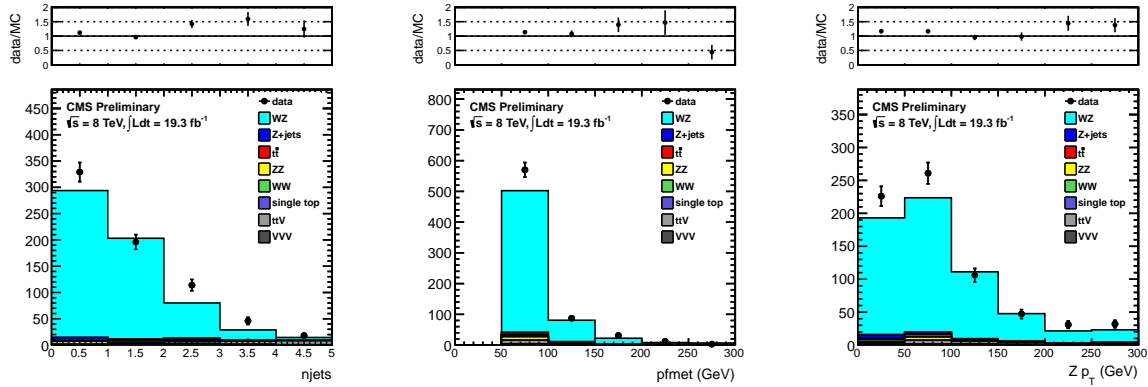| Sample	ee	$\mu\mu$	$e\mu$	total
$t\bar{t}$	1.6 ± 0.9	3.4 ± 1.5	1.8 ± 1.1	6.9 ± 2.0
$Z + \text{jets}$	1.9 ± 1.9	0.0 ± 0.0	0.0 ± 0.0	1.9 ± 1.9
WZ	40.0 ± 0.7	51.5 ± 0.7	2.7 ± 0.2	94.3 ± 1.0
ZZ	1.0 ± 0.0	1.4 ± 0.0	0.1 ± 0.0	2.6 ± 0.0
single top	0.0 ± 0.0	0.5 ± 0.5	0.0 ± 0.0	0.5 ± 0.5
WW	0.0 ± 0.0	0.0 ± 0.0	0.0 ± 0.0	0.0 ± 0.0
ttV	8.0 ± 0.4	9.5 ± 0.4	2.2 ± 0.2	19.6 ± 0.6
VVV	1.9 ± 0.1	2.6 ± 0.1	0.2 ± 0.0	4.6 ± 0.2
tot SM MC	54.4 ± 2.2	69.0 ± 1.8	6.9 ± 1.1	130.4 ± 3.1
data	87	91	22	200

Figure 8: Data vs. MC comparisons for the WZ selection discussed in the text for 19.3 fb^{-1}. The number of jets, missing transverse energy, and Z boson transverse momentum are displayed.

6.3.2 ZZ Validation Studies

A pure ZZ sample can be selected in data with the requirements:

- Exactly 4 $p_T > 20$ GeV leptons passing analysis identication and isolation requirements,

- 2 of the 4 leptons must fall in the Z window 81-101 GeV.

The data and MC yields passing the above selection are in Table 9. In this ZZ-dominated sample we observe good agreement between the data yield and the MC prediction. After requiring 2 jets (corresponding to the requirement in the analysis selection), we observe 14 events in data and the MC predicts 13.2 ± 0.2 events. Due to the limited statistical precision we assign an uncertainty of 50% on the ZZ yield.

Table 9: Data and Monte Carlo yields for the ZZ preselection.

Sample	ee	$\mu\mu$	eμ	total
ZZ	52.7 ± 0.2	73.3 ± 0.2	3.4 ± 0.0	129.4 ± 0.3
WZ	0.1 ± 0.0	0.1 ± 0.0	0.0 ± 0.0	0.3 ± 0.1
Z + jets	0.0 ± 0.0	0.0 ± 0.0	0.0 ± 0.0	0.0 ± 0.0
$t\bar{t}$	0.0 ± 0.0	0.0 ± 0.0	0.0 ± 0.0	0.0 ± 0.0
WW	0.0 ± 0.0	0.0 ± 0.0	0.0 ± 0.0	0.0 ± 0.0
single top	0.0 ± 0.0	0.0 ± 0.0	0.0 ± 0.0	0.0 ± 0.0
ttV	1.3 ± 0.2	1.4 ± 0.2	0.3 ± 0.1	3.0 ± 0.2
VVV	0.6 ± 0.1	0.8 ± 0.1	0.0 ± 0.0	1.4 ± 0.1
tot SM MC	54.7 ± 0.3	75.6 ± 0.3	3.8 ± 0.1	134.1 ± 0.4
data	56	80	5	141
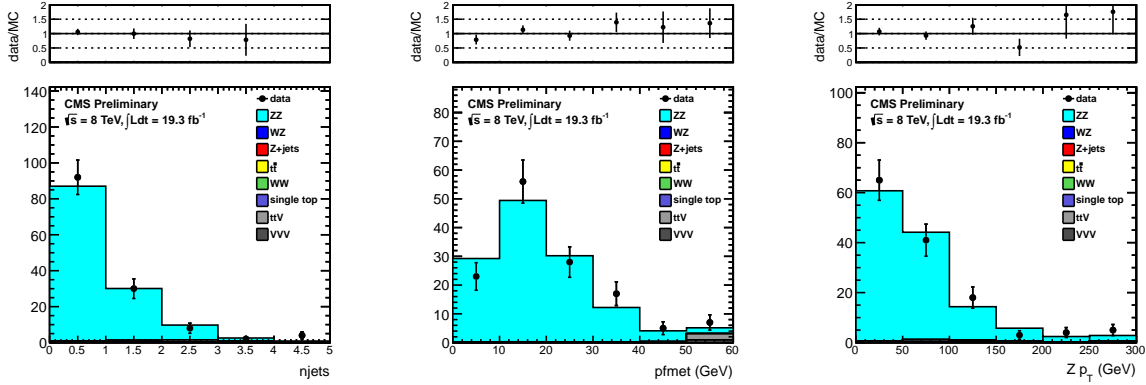
Figure 9: Data vs. MC comparisons for the ZZ selection discussed in the text for 19.3 fb^{-1}. The number of jets, missing transverse energy, and Z boson transverse momentum are displayed.

7 Results

In this section we provide the results of the inclusive and targeted searches. The observed and predicted E_T^{miss} distributions for the inclusive analysis are indicated in Fig. 10. A summary of the results in the signal regions is provided in Table 10. Good agreement is observed between the data and the predicted background over the full E_T^{miss} range.

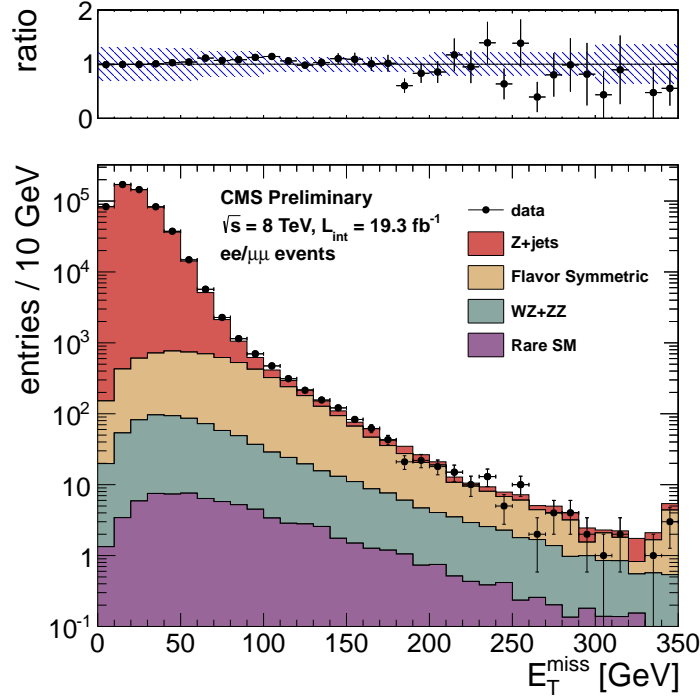Figure 10: Results of the inclusive analysis. The observed E_T^{miss} distribution (black points) is compared with the sum of the predicted E_T^{miss} distributions from $Z + jets$, flavor-symmetric backgrounds, and WZ+ZZ backgrounds. The ratio of observed to predicted yields in each bin is indicated. The error bars indicate the statistical uncertainty in the data and the shaded band indicates the total background uncertainty.

Table 10: Summary of results in the inclusive analysis. The total background is the sum of the $Z+jets$ background predicted from the E_T^{miss} templates method ($Z + jets$ bkg), the flavor-symmetric background predicted from eμ events (FS bkg), and the WZ and ZZ backgrounds predicted from MC (WZ bkg and ZZ bkg). All uncertainties include both the statistical and systematic components. The Gaussian significance of the deviation between the data and total background is indicated for signal regions with at least 20 observed events.

	E_T^{miss} 0–30 GeV	E_T^{miss} 30–60 GeV	E_T^{miss} 60–100 GeV	E_T^{miss} 100–200 GeV	E_T^{miss} 200–300 GeV	E_T^{miss} > 300 GeV
$Z + jets$ bkg	399165 ± 119750	130625 ± 39188	6652 ± 1996	266 ± 80	12.1 ± 3.8	3.0 ± 1.0
FS bkg	1031 ± 160	1948 ± 302	2056 ± 319	1022 ± 159	51.0 ± 15.1	7.4 ± 4.4
WZ bkg	128.9 ± 90.2	219.9 ± 153.9	158.2 ± 110.7	86.4 ± 60.5	11.8 ± 8.3	3.3 ± 3.3
ZZ bkg	15.9 ± 8.0	34.0 ± 17.0	36.5 ± 18.2	33.8 ± 16.9	6.8 ± 3.4	2.0 ± 2.0
rare SM bkg	10.6 ± 5.3	22.4 ± 11.2	21.9 ± 11.0	19.1 ± 9.6	3.5 ± 1.8	1.2 ± 1.2
total bkg	400351 ± 119750	132850 ± 39190	8925 ± 2025	1428 ± 189	85.3 ± 18.1	17.0 ± 6.1
data	398148	135053	9816	1507	83	7
significance	-0.0σ	0.1σ	0.4σ	0.4σ	-0.1σ	

The observed and predicted E_T^{miss} distributions for the targeted analysis are indicated in Fig. 11. A summary of the results in the signal regions is provided in Table 11. Good agreement is observed between the data and the predicted background over the full E_T^{miss} range.
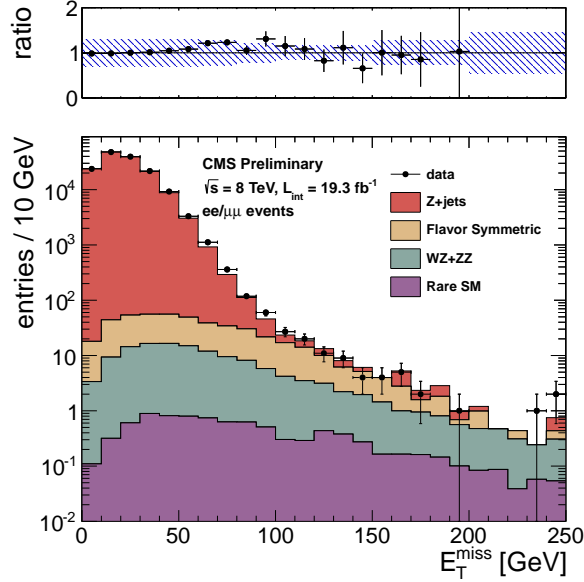

Figure 11: Results of the $Z + dijet$ analysis. The observed E_T^{miss} distribution (black points) is compared with the sum of the predicted E_T^{miss} distributions from $Z + jets$, flavor-symmetric (FS), sum of WZ and ZZ (WZ+ZZ), and rare SM backgrounds. The ratio of observed to predicted yields in each bin is indicated. The error bars indicate the statistical uncertainty in the data and the shaded band indicates the total background uncertainty.

Table 11: Summary of results in the targeted analysis. The total background is the sum of the $Z + jets$ background predicted from the E_T^{miss} templates method ($Z + jets$ bkg), the flavor-symmetric background predicted from eμ events (FS bkg), and the WZ and ZZ backgrounds predicted from MC (WZ bkg and ZZ bkg). All uncertainties include both the statistical and systematic components. The Gaussian significance of the deviation between the data and total background is indicated for signal regions with at least 20 observed events.

	E_T^{miss} 0–30 GeV	E_T^{miss} 30–60 GeV	E_T^{miss} 60–80 GeV	E_T^{miss} 80–100 GeV
$Z + jets$ bkg	111698 ± 33511	33094 ± 9929	1141 ± 343	106 ± 33
FS bkg	88.8 ± 15.0	113 ± 19	51.5 ± 8.9	38.0 ± 6.6
WZ bkg	21.5 ± 15.0	36.4 ± 25.5	15.2 ± 10.6	8.7 ± 6.1
ZZ bkg	4.6 ± 2.3	9.2 ± 4.6	4.9 ± 2.5	4.1 ± 2.1
rare SM bkg	1.0 ± 0.5	2.5 ± 1.3	1.4 ± 0.7	1.1 ± 0.6
total bkg	111814 ± 33511	33255 ± 9929	1214 ± 344	158 ± 34
data	110883	34186	1478	178
significance	-0.0σ	0.1σ	0.8σ	0.6σ
	E_T^{miss} 100–120 GeV	E_T^{miss} 120–150 GeV	E_T^{miss} 150–200 GeV	E_T^{miss} > 200 GeV
$Z + jets$ bkg	10.8 ± 3.4	6.2 ± 2.1	4.5 ± 2.6	0.5 ± 0.2
FS bkg	23.4 ± 4.2	14.0 ± 2.7	6.1 ± 2.5	0.8 ± 0.4
WZ bkg	4.7 ± 3.3	3.7 ± 2.6	2.2 ± 1.6	1.0 ± 1.0
ZZ bkg	2.4 ± 1.2	2.6 ± 1.3	1.8 ± 0.9	1.6 ± 1.6
rare SM bkg	0.6 ± 0.3	1.1 ± 0.6	0.7 ± 0.4	0.5 ± 0.5
total bkg	41.9 ± 6.5	27.5 ± 4.5	15.4 ± 4.1	4.3 ± 2.0
data	47	24	12	3
significance	0.5σ	-0.5σ		

8 Interpretation

All results in this section correspond to 9.2 fb^{-1} results and will be updated later. In this section, we interpret the results of the targeted search in the context of the WZ + E$_T^{\text{miss}}$ model depicted in Fig. 1 (right) and a gauge-mediated SUSY breaking (GMSB) model that produces a signature of ZZ + E$_T^{\text{miss}}$ will be added. The results of the targeted search presented here will be combined with those of the trilepton ewkino search for the final WZ + E$_T^{\text{miss}}$ interpretation, and with the quadlepton ewkino search for the final GMSB ZZ + E$_T^{\text{miss}}$ interpretation.

The exclusion is performed using the results of simultaneous counting experiments in the five exclusive E$_T^{\text{miss}}$ signal regions defined by E$_T^{\text{miss}} > 80$ GeV, as summarized in Table 11 (commonly referred to as a "shape analysis"). The upper limit calculation is performed with the LandS software using the LHC-type CLs criterion. The signal efficiency uncertainties include the luminosity (4.4%), acceptance for the b-jet veto (4%), lepton ID and isolation efficiency (2% per lepton), and trigger efficiency (3%). The uncertainty from JES is determined following the POG-recommended procedure, by varying the jet energies by the p_T - and η-dependent uncertainties and propagating this to the jet multiplicity, dijet mass, and E$_T^{\text{miss}}$. The background uncertainties are quoted in Table 11. For each background contribution, the uncertainty is assumed to be 100% correlated across all signal regions.

For the WZ + E$_T^{\text{miss}}$ model, the signal efficiency times acceptance and cross section upper limits are displayed in Fig. 12, along with the observed and expected exclusion contours, which are compared to the 2011 observed exclusion contour. Figure 13 shows the excluded points used to derive the exclusion contours. We note that the map of exclusion contours appears quite ragged since for many of the points the cross section upper limit is very close to the theory cross section. Therefore we do not expect the ragged exclusion region to be an issue for the final results since we currently have 9.2 fb^{-1} and expect the luminosity to increase significantly. A **VERY APPROXIMATE** projection of the expected excluded region for an integrated luminosity of 15 fb^{-1} (a rough guess at the final HCP data sample) is obtained by scaling the expected cross section limits by $\sqrt{(9.2\text{fb}^{-1})/(15\text{fb}^{-1})}$, as displayed in Fig. 14.
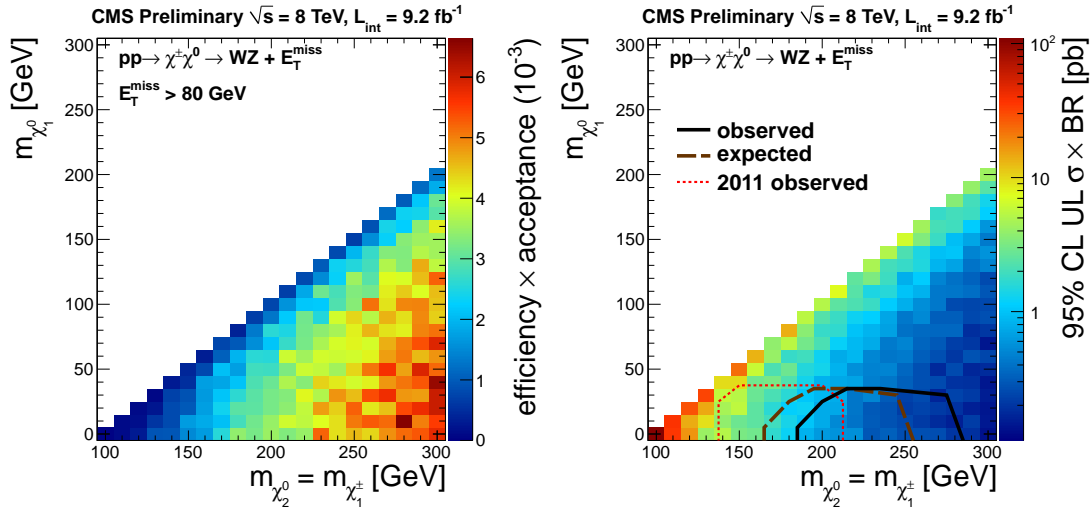

Figure 12: Interpretation of the targeted analysis in the WZ + E$_T^{\text{miss}}$ model. The acceptance times efficiency (left) and cross section upper limit (right) are displayed. The observed and expected exclusion contours are indicated and compared to the observed exclusion from the 2011 analysis.
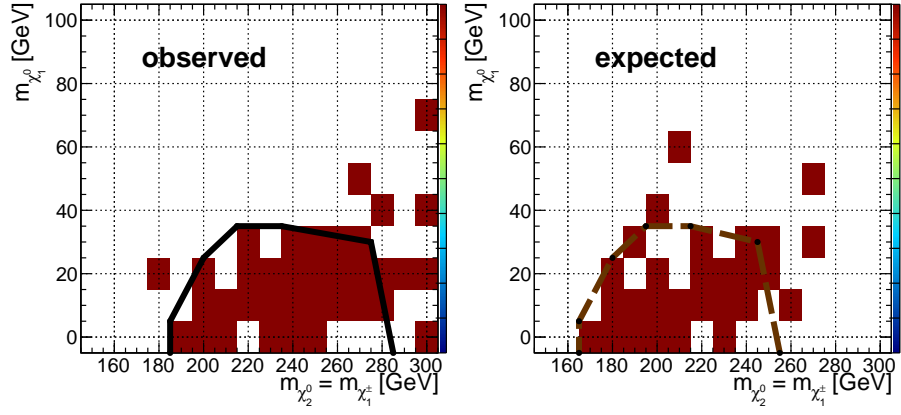
Figure 13: Observed (left) and expected (right) excluded points for the $WZ + E_T^{miss}$ interpretation, with the corresponding exclusion contours overlaid.
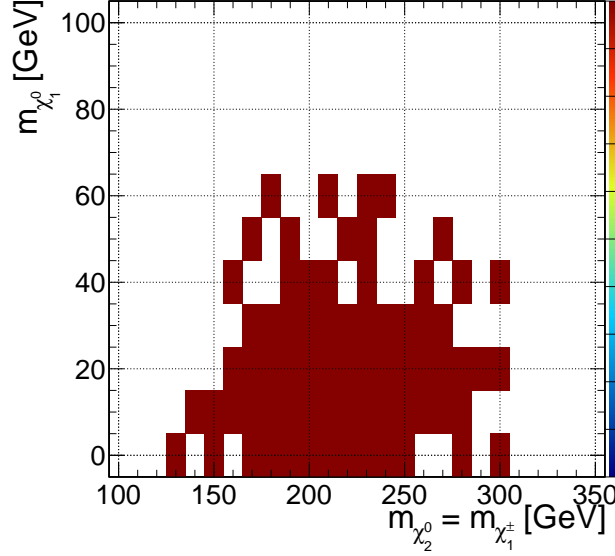
Figure 14: A **VERY APPROXIMATE** projection of the expected excluded points for an integrated luminosity of 15^{-1}.

The results of the interpretation in the GMSB $ZZ + E_T^{miss}$ model are displayed in Fig. 15, as a function of the chargino and neutralino mass parameter μ. These results exclude the range $196 < \mu < 316$ GeV.
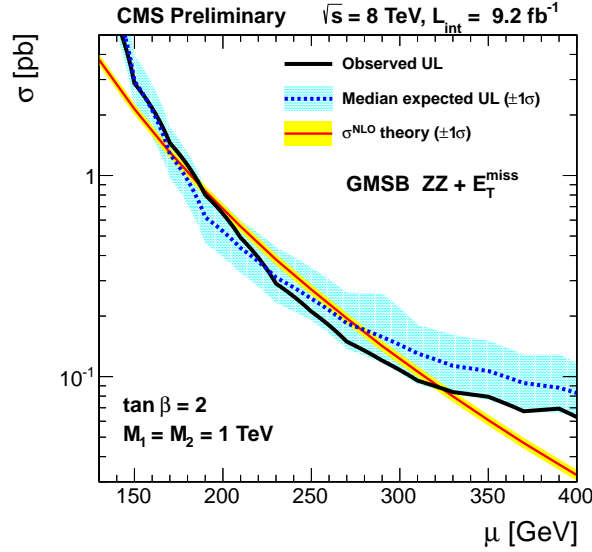

Figure 15: Interpretation of the targeted analysis in the GMSB $ZZ + E_T^{miss}$ model.

9 Summary

This note presents a search for BSM physics in final states with leptonically-decaying Z bosons, jets, and E_T^{miss}. Two strategies were pursued. The first is an inclusive approach which targets BSM scenarios with Z bosons produced in the decays of strongly-interacting particles. The second is a targeted approach which focuses on BSM scenarios where the Z bosons are produced in the decays of weakly-interacting particles. The main backgrounds are estimated with data-driven techniques. Good agreement is observed between the data and the predicted backgrounds over the full E_T^{miss} range, for both searches. The results are interpreted in the context of a simplified SUSY model where chargino-neutralino pairs decay to the $WZ + E_T^{miss}$ final state, and used to place constraints on the masses of these particles.

Table 12: Summary of the parameters for the GMSB model used for the $ZZ + E_T^{\mathrm{miss}}$ interpretation. The masses of the lightest and second light neutralino, lightest chargino, and total next-to-leading order cross section, are indicated.

μ [GeV]	$m_{\tilde{\chi}_1^0}$ [GeV]	$m_{\tilde{\chi}_2^0}$ [GeV]	$m_{\tilde{\chi}_1^\pm}$ [GeV]	σ_{NLO} [pb]
130	122	131	124	3.8
150	141	151	144	2.1
170	161	171	164	1.3
190	181	191	184	0.84
210	201	211	203	0.56
230	221	231	223	0.38
250	240	251	243	0.27
270	260	271	263	0.20
290	280	291	283	0.14
310	299	311	302	0.11
330	319	331	322	0.080
350	339	351	342	0.061
370	358	371	362	0.047
390	378	391	381	0.037
410	398	411	401	0.029

References

[1] CMS Collaboration, "Search for physics beyond the standard model in events with a Z boson, jets, and missing transverse energy in pp collisions at $\sqrt{s} = 7$ TeV,", arXiv:1204.3774v1 [hep-ex].

[2] SUS-12-006, paper draft

[3] https://twiki.cern.ch/twiki/bin/viewauth/CMS/EgammaCutBasedIdentification

[4] https://twiki.cern.ch/twiki/bin/viewauth/CMS/EgammaEARhoCorrection

[5] https://twiki.cern.ch/twiki/bin/view/CMSPublic/SWGuideMuonId

[6] M. Chen, AN 2012/237 "Interpretation of the Same-Sign di-leptons with bjets and MET search"

A WZ Kinematic Distributions

All results in this section correspond to 9.2 fb^{-1} results and will be updated later. As discussed in Sec. 6.3.1, we observe an excess of events with 3 isolated leptons and at least 2 jets ($3\ell+ \geq 2$ jets sample). In this section we compare some basic kinematic distributons in data vs. MC for these events. As stated in Table 8, we observe 98 data events and predict 59 ± 1.4 (stat) events (from pure MC) in the ee+$\mu\mu$ channel. Since we are interested in comparing the shapes of kinematic distributions, we normalize the MC to match the data yield by applying a scale factor of 1.66 to the MC.

A comparison of the transverse mass of the non-Z lepton and the $\mathrm{E_T^{miss}}$ (M_T) and the $\mathrm{E_T^{miss}}$ are displayed in Fig. 16. An excess of events with large M_T would be inconsistent with WZ production. We count evens with $M_T > 100$ GeV and find 19 events in data, with an MC prediction of 14 ± 0.9 (after applying the 1.66 scaling factor); hence we do not observe evidence for a significant excess at large M_T. Data vs. MC comparisons of lepton p_T are displayed in Fig. 17, hadronic variables (jet multiplicity, H_T, and number of b-tags) are displayed in Fig. 18. All distributions show reasonable data vs. MC agreement; hence we do not observe kinematic distributions which are inconsistent with WZ production.
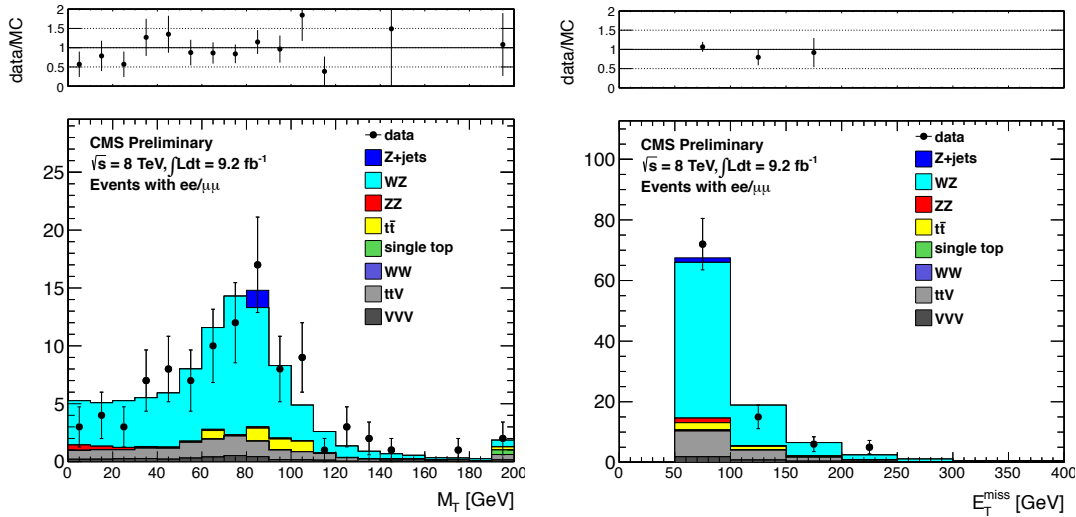

Figure 16: Data vs. MC comparison of the M_T (left) and $\mathrm{E_T^{miss}}$ (right) distributions for the $3\ell+ \geq 2$ jets sample.
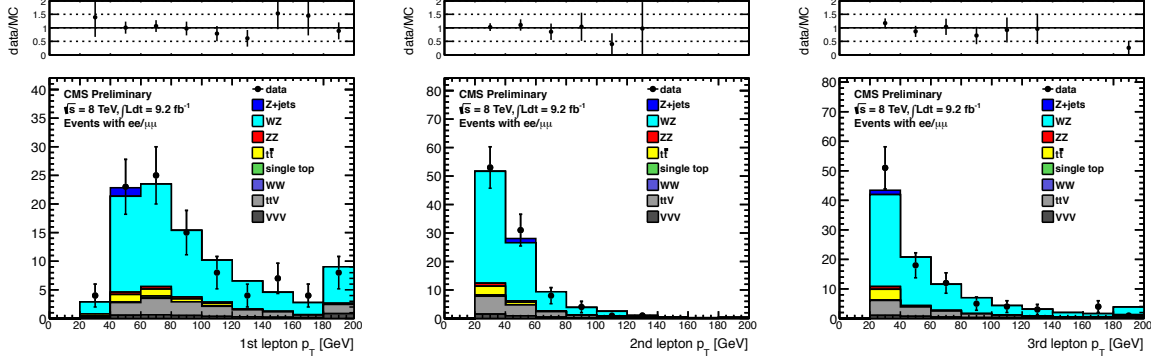
Figure 17: Data vs. MC comparison of the 1st (left), 2nd (middle) and 3rd (right) lepton p_T distributions for the $3\ell+ \geq 2$ jets sample.
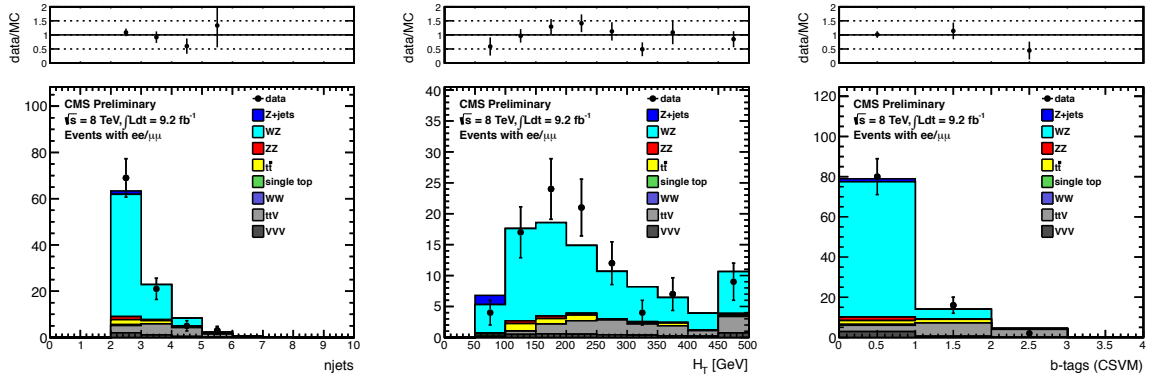

Figure 18: Data vs. MC comparison of the jet multiplicity (left), H_T (middle), and number of b-tags (right) distributions for the $3\ell+ \geq 2$ jets sample.

B E_T^{miss} **Templates from** $\gamma + \text{jets}$ **Sample**

In this section we display the templates used for the inclusive analysis (red) and the targeted analysis (blue).
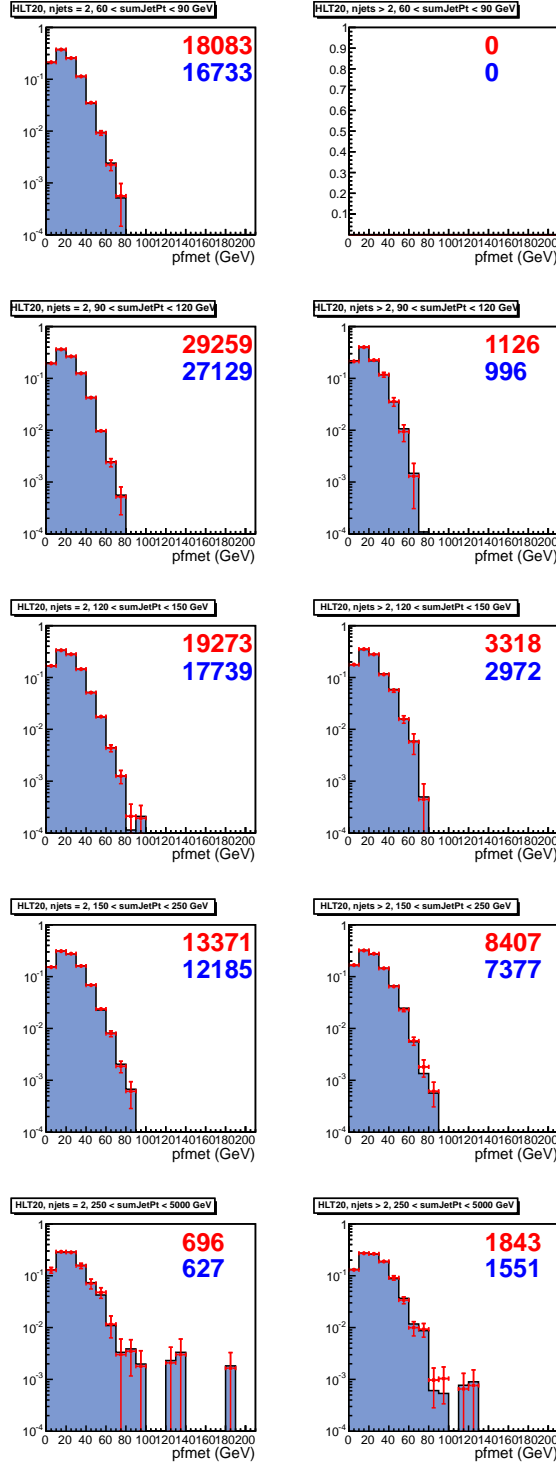
Figure 19: E_T^{miss} templates collected with the $p_T > 22$ GeV single photon trigger. The number in red (blue) indicates the number of entries in the template for the inclusive (targeted) analysis.
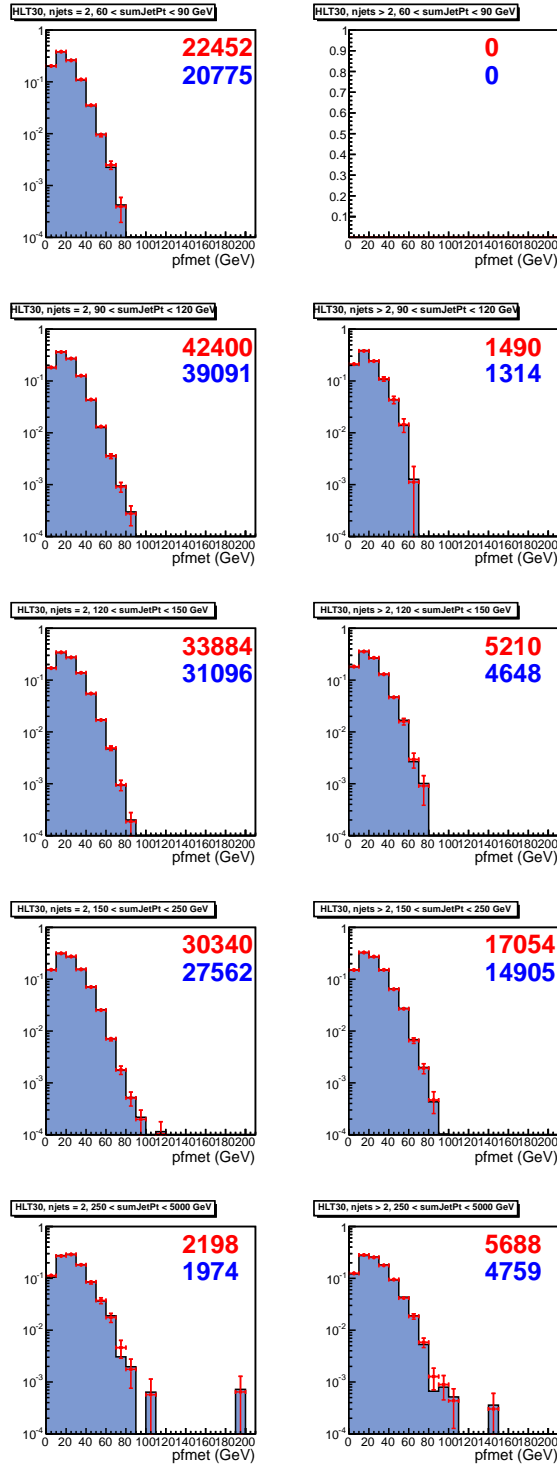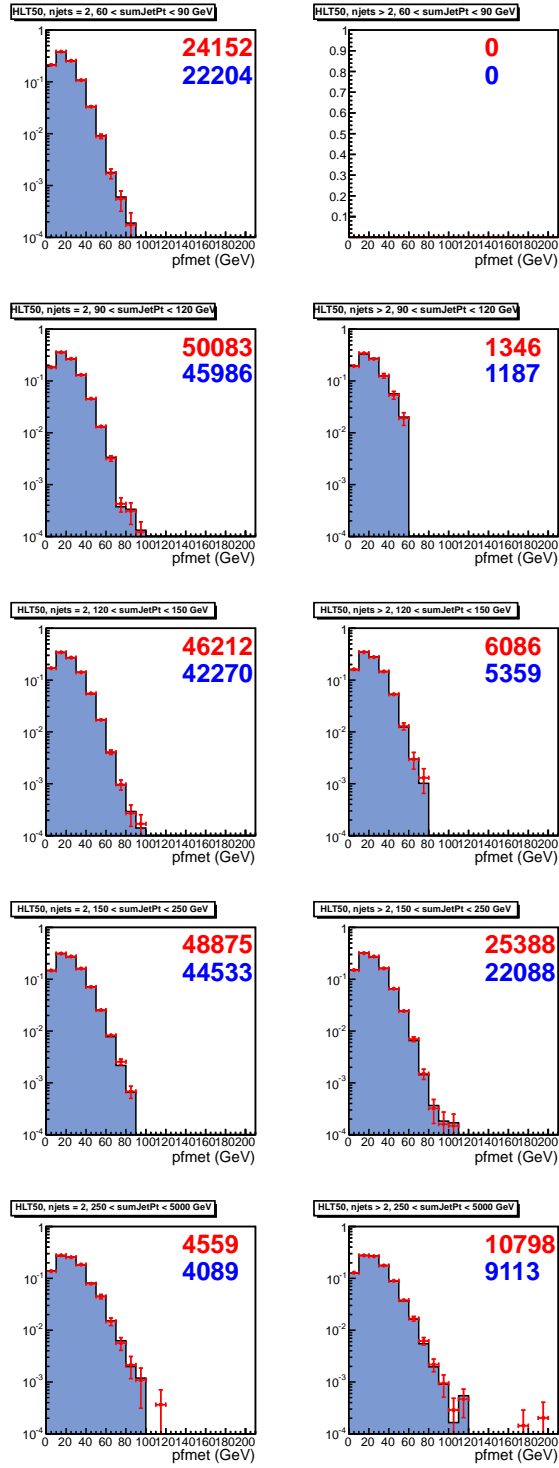
Figure 20: E_T^{miss} templates collected with the $p_T > 36$ GeV single photon trigger. The number in red (blue) indicates the number of entries in the template for the inclusive (targeted) analysis.

Figure 21: E_T^{miss} templates collected with the $p_T > 50$ GeV single photon trigger. The number in red (blue) indicates the number of entries in the template for the inclusive (targeted) analysis.
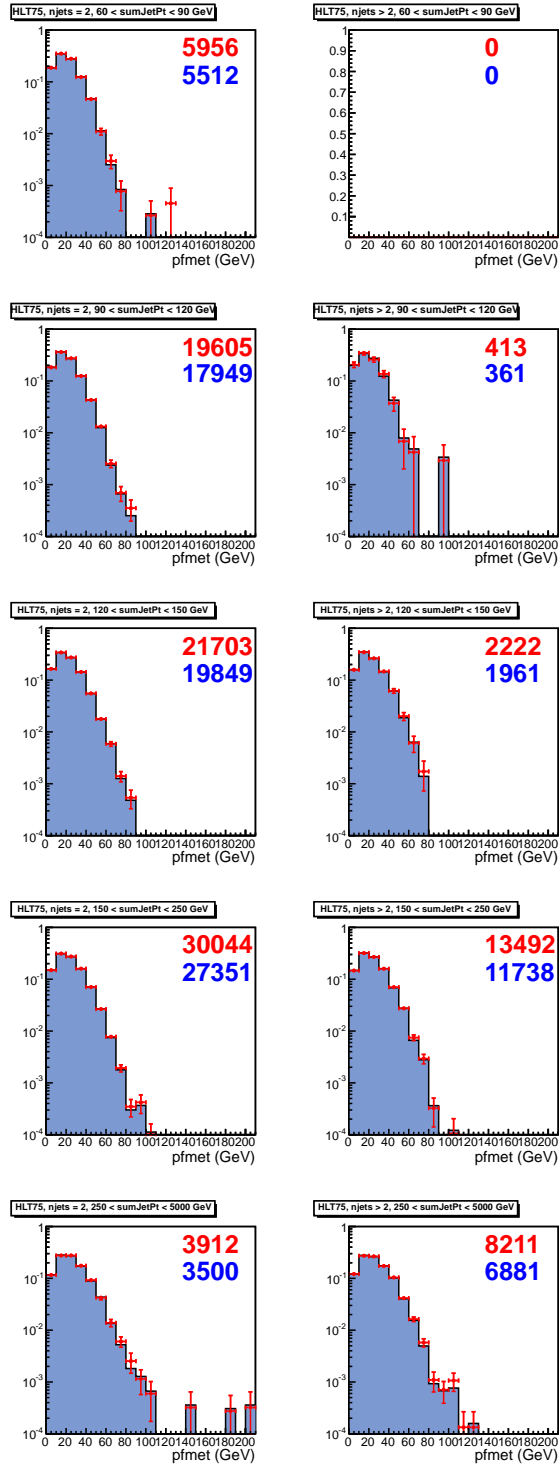
Figure 22: E_T^{miss} templates collected with the $p_T > 75$ GeV single photon trigger. The number in red (blue) indicates the number of entries in the template for the inclusive (targeted) analysis.
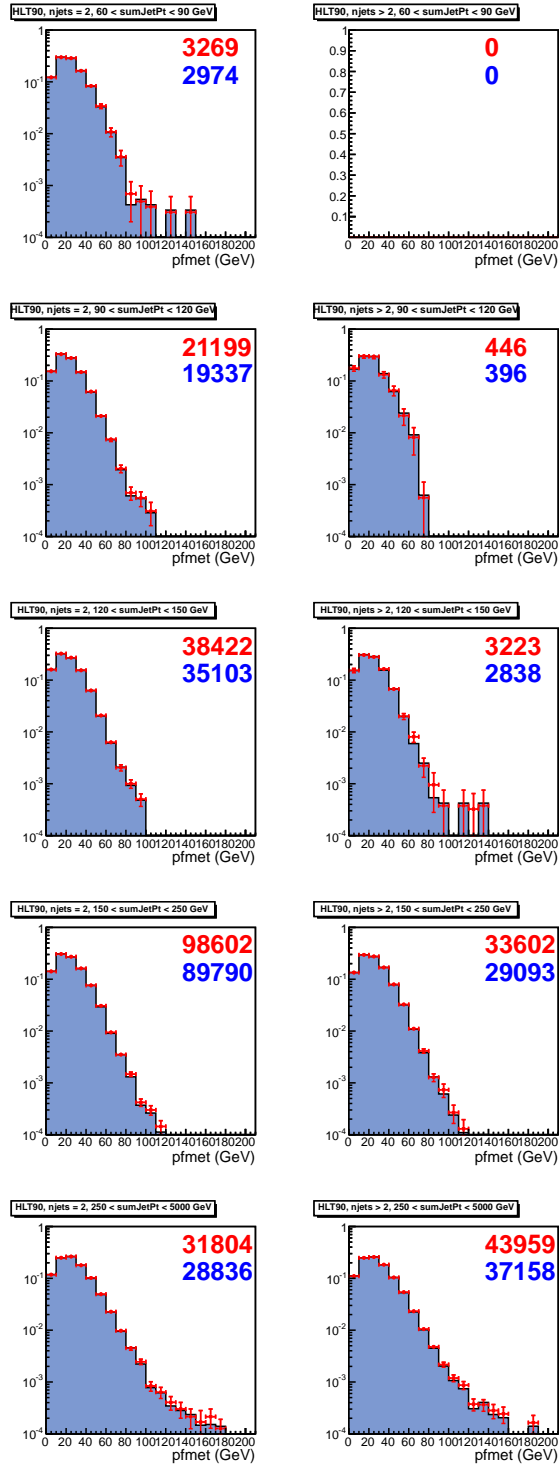
Figure 23: E_T^{miss} templates collected with the $p_T > 90$ GeV single photon trigger. The number in red (blue) indicates the number of entries in the template for the inclusive (targeted) analysis.